

Energy Management Strategy of Stand-alone Photovoltaic System in Cathodic Protection Pipeline

J. Javidan*

Department of Electrical Engineering, University of Mohaghegh Ardabili, Ardabil, Iran.

Abstract- In this paper, the stand-alone photovoltaic system for cathodic protection of underground pipelines is presented. The proposed system offers continuous and automatic adjustment of the applied voltage so that the buried pipelines receive the exact current. A modified perturb and observe (P&O) algorithm for maximum power point tracking (MPPT) is used to improve dynamic and steady state performance. The battery stores excess energy generated by PV array and supplies the load when there is a shortage of the photo voltaic (PV) power. To extend the battery lifetime and the system efficiency, the battery is connected to the DC link by a ZVS bidirectional Buck-Boost converter. A classic PI controller regulates output voltage by controlling the duty cycle of the converter. The supervisor controls the converter to operate system in suitable modes based on the state of charge (SOC) of the battery and DC link voltage. The simulation verified that the output voltage obtains the constant voltage under any climatic conditions.

Keyword: DC-DC converter, Photovoltaic, Maximum power point tracking, Anode-bed, Cathodic protection.

1. INTRODUCTION

Corrosion is a malicious chemical or electrochemical reaction between the metal surface and the surrounding environment. However, a variety of coatings are used in underground steel pipes (water, gas, oil), but still oxidation process occurs and causes corrosion in pipes and destroys them. In cathodic protection technique, the under corrosion pipeline acts as the cathode and the pipeline connects to a DC power source or a sacrificial metal which acts as the anode. Cathodic protection can be applied to the naked surfaces of the steels, but it is often uneconomical because the current density flows in steel to protect from corrosion is very high. The combination of appropriate coating and cathodic protection may be the best recommended method in the practical realization of the pipe protection. The cathodic protection may be realized either by current injection technique, called impressed current cathodic protection, or sacrificial anode, called passive cathodic protection [1]-[3].

A typical method for the realization of a DC power source to provide protection is often used a transformer-rectifier connected to AC power. In the absence of an AC

supply, alternative power sources may be used, such as solar panels, wind power or gas powered thermo-electric generators [4]. In comparison with conventional systems that inject current by using a rectifier transformer, solar smart cathodic protection system has several advantages. For example, the construction and installation costs of the smart system are lower than that of the conventional systems. The conventional system needs a balanced three-phase electrical system, but the smart system uses clean solar energy. It may be found two main methods in the literature for implementing solar cathodic protection system. In the first method, Photovoltaic (PV) array is connected to storage battery by using a battery voltage regulator circuit. The storage battery supplies the load with the required voltage under varying climatic conditions by using load voltage regulator circuit. The selector and feedback circuit is designed to keep the test point always constant regardless of the climatic and soil variations. In the second method, two converters are used in series to connect photovoltaic (PV) array to the load. The storage battery is connected between the two converters, called a DC link, by a bidirectional DC-DC converter. In this paper, the second method has been adopted [5-6].

The generated power of the solar modules covers a wide range power because of the variation of the level of solar irradiation and the temperature of the solar cells. To make better use of the obtained solar energy, the system needs the maximum power point tracking (MPPT) controller to be able to take maximum power from the solar modules. In recent years, several MPPT techniques

Received: 3 Jan. 2016

Revised: 13 May 2016

Accepted: 12 June 2016

*Corresponding author:

E-mail: javidan@uma.ac.ir (J. Javidan)

have been proposed in the literature; such as Constant Voltage (CV), Perturb and Observe (P&O), Incremental Conductance (IC), Fuzzy Logic, and Artificial Neural Network method [7]. P&O algorithm is an iterative method to find the maximum power point and has been widely used because its realization needs simple control circuit and less measured parameters. The reaction of this algorithm is weak when a sudden change occurs in brightness. Refs. [7]-[10]. Because of less complexity and simple control circuit, in this paper, we used a modified P&O algorithm in the realization of MPPT block.

The way that the power management controller controls the energy flow in a hybrid system defines how the system operates and how its vital variables change. There have been a number of studies of power management strategies in the literature [11-15]. Generally, the management strategy of power systems is classified into three categories; centralized control arrangement, distributed control arrangement, and hybrid centralized and distributed control arrangement. In all three categories, each renewable energy resource has its own local controller that determines the optimal operation of the unit based on the current information.

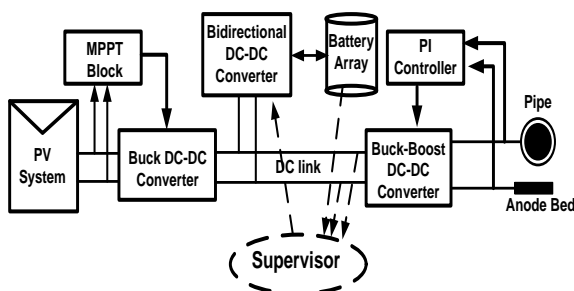


Fig. 1 Block diagram of the intelligent solar cathodic protection

In centralized control arrangement, the entire system comprised of one master controller (centralized controller) and several slave controllers for various renewable energy resources and energy storage system. In distributed control arrangement, each energy source sends measurement signals to its local controller. The local controllers communicate with one another to take appropriate decision for global optimization. Hybrid control arrangement is the combination centralized and distributed control schemes. In this study, the centralized control arrangement is used.

This paper is organized as follows: In Section 2, stand-alone system is described, Section 3 the modeling of the system components introduce with more detail. Section 4 includes description of the proposed power management strategy. Optimal sizing of PV system is given in section 5. Simulation results are shown in section 6 and section 7 concludes the works.

2. STAND-ALONE SYSTEM DESCRIPTION

Stand-alone PV systems are designed to operate independent of the electric utility grid, and are generally designed and sized to supply certain DC and/or AC electrical loads. The simplest type of stand-alone PV system is a direct-coupled system, where the DC output of a PV module is directly connected to a DC load. In direct-coupled systems, the load only operates during sunlight hours. The most common applications for this system are such as ventilation fans, water pumps and small circulation pumps for solar thermal water heating systems. In some stand-alone PV applications, electrical power is required from the system during the night or hours of darkness. Thus, the storage must be added to the system. Generally, batteries are used for energy storage. Several types of batteries can be used such as lead-acid, nickel-cadmium and vanadium batteries. Different factors are considered in the selection of batteries for PV application [16]-[18].

Figure 1 shows the power converter framework of the stand-alone PV system. The system is mainly composed of a PV module, a maximum power point tracking (MPPT) controller, a battery bank, a buck converter, a bidirectional buck-boost converter, a unidirectional buck-boost converter, pipeline with the anode bed and central supervisor. The operation mode of the studied system is as follows: In regular operation, the wide-range voltage of the solar cell is converted to lower voltage both by a unidirectional DC/DC Buck converter and by an MPPT controller. A unidirectional buck-boost converter connected serially to the buck converter provides load energy because it has the capability to step-up and step-down the input voltage. The excess energy from the PV above the hourly demand is stored in the battery until the battery is fully charged. The battery is discharged when the PV is fully or partially shaded and the load demand is higher than the generated energy. Therefore, a bidirectional buck-boost converter may be employed for charging and discharging the battery. A central control unit or supervisor acquires the required voltage and current necessary to assess the operational state of the different blocks and provides control references for the operation of several converters. Control algorithms in cooperation with the control unit define the converters control signals. In this study, control unit according to control strategy is programmed to maintain a constant voltage between pipeline and anode bed. In addition, the control unit coordinates the bidirectional buck-boost converter to charge and discharge the batteries and to protect the batteries, avoiding both the risk of overcharging and the reach of an excessive discharge level.

3. MODELLING OF SYSTEM COMPONENTS

3.1. PV Modelling

A group of PV cells connected in series to provide a significant voltage is called a PV module. Series or parallel combinations of PV modules form a solar panel, and again, a group of PV panels results in a PV array. Naturally, PV module exhibits a nonlinear current-voltage (I-V) and power-voltage (P-V) characteristics that vary with the radiation intensity and cell temperature. Since the PV module has nonlinear characteristics, the equivalent circuit model of a PV cell is needed in order to simulate its real behaviour of PV system applications. One of the models proposed in literature is the two-diode mode and we used this model for PV modules in Matlab/Simulink to simulate the total system [19]. An applied solar panel in this study is collection of six modules of the polycrystalline silicon from Faran Company [20] connected in three parallel rows with two modules in series with maximum power of 1770 W.

3.2. Buck converter

The main purpose of the Buck converter is to convert the DC input from the PV into a lower DC output [21]. The maximum power point tracker uses the Buck converter to adjust the PV voltage at the maximum power point. A buck type converter steps down the PV voltage to low voltage necessary for the battery and the buck-boost converter.

3.3. MPPT Controller unit

When dealing with alternative sources of energy, the search for the point of maximum power becomes more important than the maximum efficiency. In order to ensure the maximization of the power extracted from the PV source, the interface power converter must be capable of self-adjusting its own parameters at run time. The control parameter of the converter is the duty cycle D of the main switch and must be changed continuously by a controller to ensure that the PV generator always operates at its maximum power point (MPP) for whatever irradiance and temperature operating conditions. According to Fig. 2, if a load R_{LA} is connected directly to a PV module, the operating point will be at A. When the load increases to R_{LC} , the operating point will move to C. During this range of load variation, there is only one point at which the PV module provides its MPP. This point is when the load resistance equal to the resistance at MPP ($R_L = R_{opt}$), (point B). However, it is very difficult to select a fixed load, which matches this value, and even if this is done, this point itself changes under changed climatic conditions. On the other hand, when a DC-DC converter is connected between the PV module and the load, the operating point depends on the impedance seen by the

module (R_{in}), which depends on two parameters: R_L and duty cycle (D). Thus, under different loads, the duty cycle can be adjusted to change R_{in} to match R_{opt} at any atmospheric conditions. Assume that the buck converter operates in CCM, with duty cycle D_1 and the buck-boost converter operates in CCM, with duty cycle D_2 . The average input impedance R_{in} for Buck converter is $R_{in} = R/D_1^2$ and for Buck-Boost converter is

$$R_{in2} = \frac{(1-D_2)^2}{D_2^2} R .$$

Therefore, the average input impedance seen by PV Module in the proposed structure

$$\text{is } R_{in} = \frac{1}{D_1^2} \frac{(1-D_2)^2}{D_2^2} R .$$

The equation indicates that the cascaded Buck converter with buck-boost converter can match any output load to the optimal PV impedance and does not have constraining limits. It is also possible a cuk converter instead of buck-Boost converter to do same function [22].

By investigating the Power-Voltage relationship of a typical PV module shown in Fig.2, The perturbation and observation (P&O) method is the most popular algorithm belonging to the class of the direct MPPT techniques. This algorithm involves a perturbation in the operating voltage of the PV array, and then if change of power (ΔP) is positive, the future perturbation should be kept the same to reach the MPP and if change of power (ΔP) is negative, the direction of perturbation should be reversed to move back toward the MPP. Therefore, the perturbation size is reverted to force the operating point back to the true MPP. This process continues until the algorithm reaches the point of maximum power. Then swing around to this point. We modified P&O algorithm similar to the methods proposed in Ref. [23]. It has been shown that P&O algorithm with the variable step size would be improve dynamic and steady state performance of the MPPT system.

3.4. Unidirectional Buck-Boost converter

The output voltage of the Buck-Boost converter can be higher and lower than the input voltage [21]. By considering that the output voltage in the cathodic protection system changes over time and when the coating of the pipe is new and the sacrificial anodes have lower resistance, thus in the early installation, low power consumption is required.

However, over time, coatings and anodes lost their property, so the power consumption, too, will increase and correspondingly, the output voltage is increased.

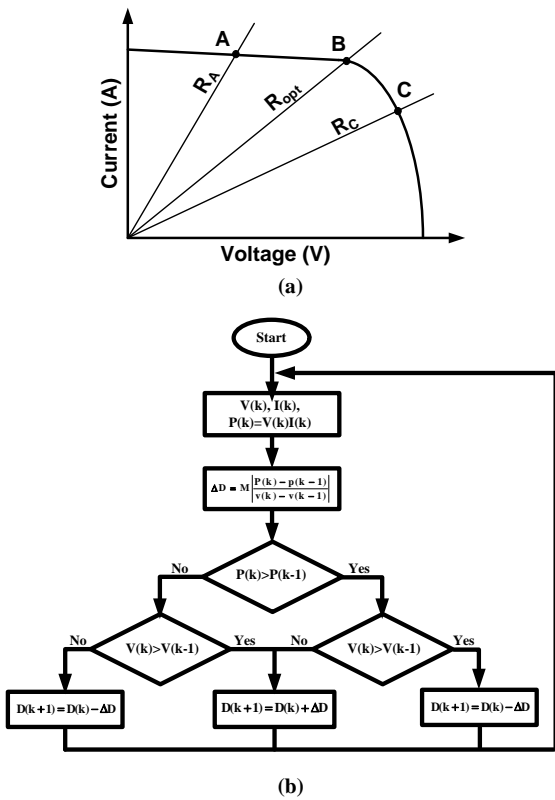


Fig. 2 (a) Location of operating point of a PV module with a variable resistive load (b) Flowchart of modified P&O method

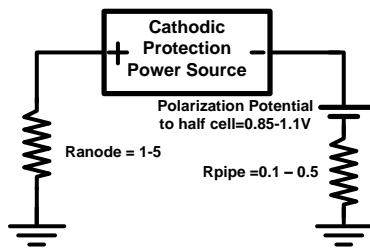


Fig. 3. Equivalent circuit of pipeline and ground bed

3.5. Equivalent circuit of the pipeline and the anode-bed

The parameters of the equivalent circuit of the pipeline in cathodic protection can be found in Ref. [24]. The equivalent model of a pipeline with the anode bed can be modelled as shown in Fig. 3. The main purpose of the design is to control drain point voltage (V_{dp}). Drain point voltage should be controlled on a constant value. Where, this value depends on the type of the coating and the voltage at the end of the transmission line. According to national Iranian gas company standard and national American corrosion standards (NACE), drain point voltage should set at -1.5v for cold coating, -2.1v for warm coating and -1.2v for three-layer polyethylene coating. Generally, this value can vary between -0.85v and -2.1v with respect to the conditions of the transmission lines.

3.6. Battery

To facilitate power storage generated from stand-alone photovoltaic systems during overproduction, it provides the stored power as an auxiliary service during electricity shortages. In some previous applications, the battery-bank is directly connected to a DC bus without a bidirectional converter. This configuration requires high voltage batteries or more battery stacks and reduces the system efficiency. Refs. [25]-[26]. This study proposes a bidirectional buck-boost converter to manage the storage and supply of power between photovoltaic power generation systems and batteries. Bidirectional DC-DC converter allows transfer of power between two DC sources, in either direction, while maintaining the voltage polarity and value at either end unchanged.

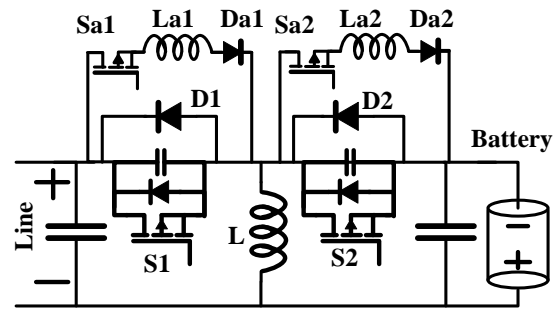


Fig. 4. Bidirectional buck-boost converter

Therefore, it is possible to use low voltage batteries to charge/discharge management. A charge/discharge control strategy must keep the battery in the highest possible state while protecting it from overcharge by the photovoltaic generator and from over-discharge by loads. Because of overcharging and undercharging batteries will produce hot spots inside the battery such that the batteries not survive for a long time. The battery state of charge (SOC) would be adjusted to match the power demand of the load. For this reason, if the battery SOC is below 90% and there is sufficient power from the PV module to charge the battery, then the bidirectional converter charges the battery. On the other hand, if the battery SOC is above 10% and the load needs support from the battery, then the bidirectional converter delivers power from the battery to the load. Whenever the battery is overcharged or has no sufficient charge to deliver, then it automatically goes to the waiting mode. In this design, we used several 24 V- 1200 Ah industrial batteries from Sababattery Company [27].

3.7. Bidirectional Buck-Boost converter

This study proposes a bidirectional buck-boost converter as shown in Fig. 4 to manage the storage and supply of power between photovoltaic power generation systems and batteries. The proposed interface circuit is shown in Fig. 4. This bidirectional converter operates in two modes

of operation: (1) it acts as a ZVS Buck/Boost to charge battery (2) it acts as a ZVS Buck/Boost to discharge the battery. During charge operation mode, S1 and D₂ are on while during the discharge mode, S2 and D₁ are on. In addition, the auxiliary circuit is connected in parallel to the active switches and provides the soft switching condition for S1 and S2 while La1 provides ZC condition for Sa1 turn on and La2 provide ZC condition for Sa2 turn on. The auxiliary circuit is composed of an auxiliary switch (S_{a1}, S_{a2}), a series diode (D_{a1}, D_{a2}) and a resonant inductor (L_{a1}, L_{a2}). The proposed converter in charge operation is shown in Fig. 4. The converter theoretical waveforms are shown in Fig. 5a. During one switching cycle, the proposed converter has six operating intervals or modes. Also, the proposed converter in discharging operation is shown in Fig. 4. The converter theoretical waveforms are shown in Fig. 5b. During one switching cycle, the proposed converter has six operating modes.

The basic principle behind the ZVS operation of the converter is that the auxiliary switch, S_a, is turned on just before the main switch is turned on. The resonant loop of the resonant inductor (L_{a1}), a diode Da1 and the output capacitance across the main switch is completed by the turning ON of the auxiliary switch. By the help of resonance, the auxiliary switch is made to operate at ZCS.

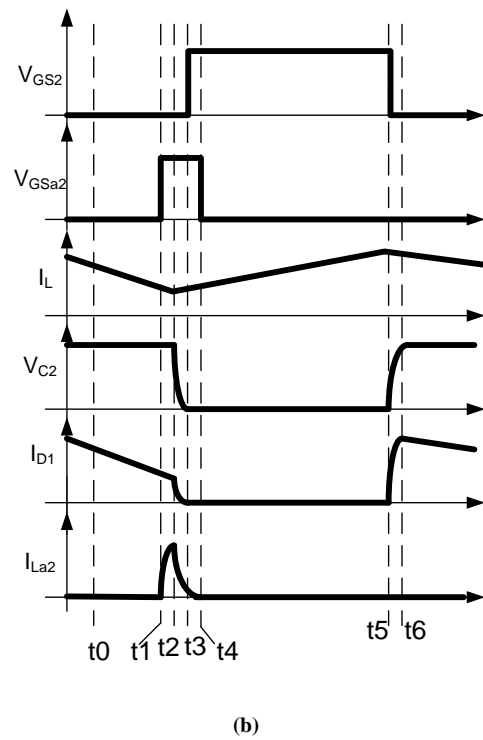
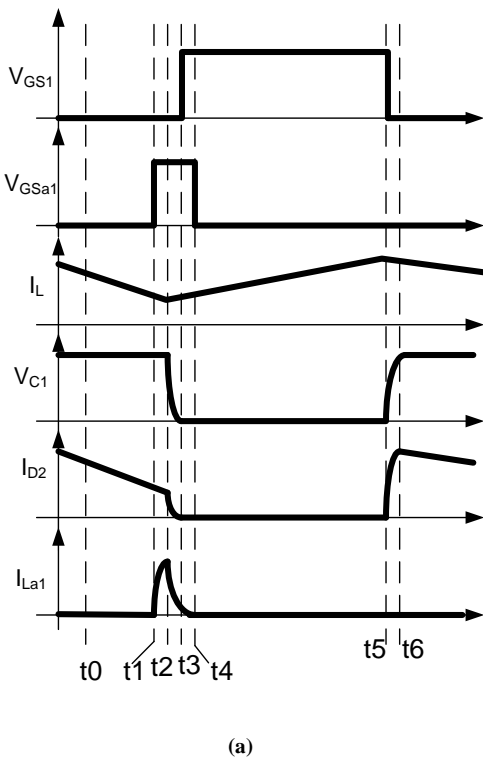


Fig. 5 (a) Waveforms of the converter at charging mode (b) Waveforms of the converter at discharging mode

The auxiliary inductor current linearly increases and the output capacitance across the main switch starts discharging. As the parasitic capacitor is discharged the current in the resonant loop flows through the anti-parallel diode of the main switch. By turning ON the main switch, the ZVS is assured.

4. POWER MANAGEMENT STRATEGY

The configuration of the stand-alone PV system, used in this paper to meet the power demanded by pipeline to protect pipeline from corrosion, is shown in Fig. 1. In this system, the primary energy source is the PV arrays and the backup and storage system is the battery. Four controllers and one supervisor are involved in the system. The first controller is MPPT controller to extract maximum power from PV modules.

The second controller is the classic PI controller, which controls the bidirectional DC/DC converter duty cycle during the battery-charging mode. The third controller is the classic PI controller, which controls the bidirectional DC/DC converter duty cycle during the battery-discharging mode.

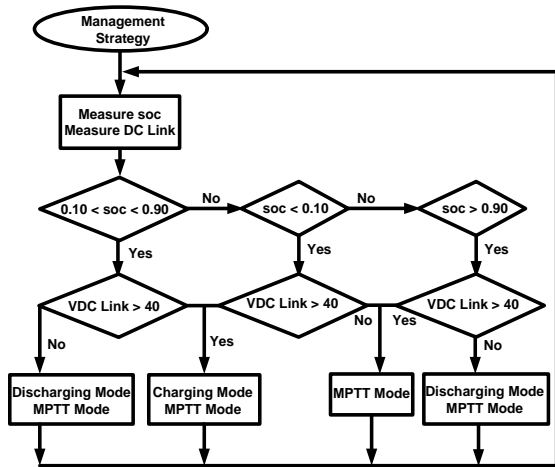
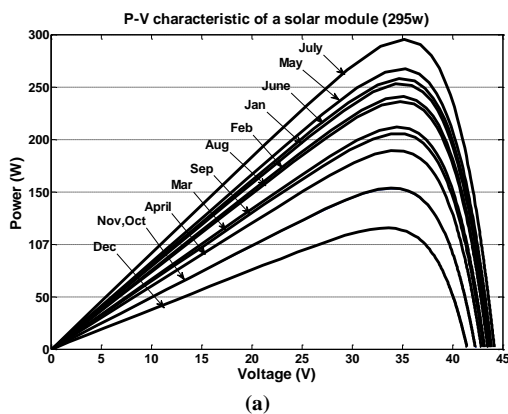


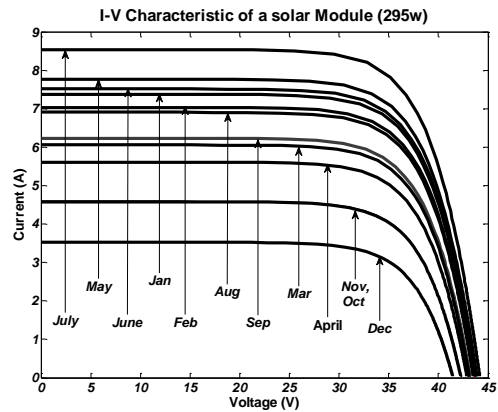
Fig. 6 Flowchart of the PV System management strategy

The last classic PI controller is used to track drain point voltage V_{DP} reference on the load side for the unidirectional Buck-Boost converter located between DC Link and the load.

The main decision factors for the power management strategies are the level of the power provided by the renewable energy system (solar) and the state of charge (SOC) of the battery bank. The battery bank or the fuel cell should be capable of providing the needed power. Power energy generated by PV panels is summed up at renewable energy system power. Besides the load demands, any excess power which is the difference between the PV output power and the load demand should be directed into the energy storage system. The power management strategy should determine the power dispatch between the renewable energy sources, the energy storage device, and the DC load. The control strategy of the system can be divided into four operational modes based on the PV power, the DC link, the V_{DP} value, and the SOC of the battery, which is described as follows.



(a)



(b)

Fig. 7. (a) P-V characteristic of a solar module 295w, (b) I-V characteristic of a solar module 295w

Mode I: When the light gradually increases and the maximum power of PV modules is greater than the load demand and the DC link voltage is greater than 40V. The DC/DC converter for PV modules works with MPPT mode. If the battery has not been fully charged, $SOC < 90\%$, the supervisor turns on the controller in charge mode. Therefore, the bidirectional DC/DC converter for the battery works and is used to charge the battery and the battery will absorb the excess energy. The overcharging and over current of a battery is avoided by putting a limiter in the converter.

Mode II: When the light further increases and the power output of PV modules are far higher than the load power, in the first the DC/DC converters for PV modules work with MPPT. If the battery has been fully charged, $SOC > 90\%$, the supervisor turns off the controller in charge mode.

Mode III: when PV modules cannot provide enough energy to power the load, DC Link is not in normal range in the case of overcast sky or at night. PV modules work in an MPPT mode to maximize solar energy and the supervisor turns on the controller in discharging mode. Therefore, the shortage will be compensated by the battery discharging via the bidirectional buck/boost converter.

Mode IV: Due to continuous raining days during the operation mode III, the battery may come into over-discharge state for continuously supplying power to the load. When the battery voltage reaches over-discharged-point voltage ($SOC < 10\%$), the supervisor turns off the bidirectional Buck/Boost converter controller immediately to protect the battery, and only PV modules work with MPPT and provide load demand. A flowchart of the management strategy of the PV system is depicted in Fig. 6.

5. OPTIMAL SELECTION OF PV SYSTEM

In order to ensure acceptable operation at minimum cost, it will be necessary to determine the correct size of each element. It is noted that the design should be done on meteorological data, solar irradiance and on the exact load consumption over long periods. To design the entire solar cathodic protection system, the project lifetime is assumed twenty years and the worst case producing power condition is considered. The number of PV modules and the capacity of the battery and converter specifications are calculated based on the daily power consumption of the pipeline. Table 1 shows the measured data obtained from the output voltage and current of the rectifier transformer in Razei station of IRAN during a 9-year period. Therefore, in one day the load will consume $(5.56 \times 37.5 \text{ watts}) \times (24 \text{ hours}) = 5.004 \text{ kWh}$ of electrical energy. The output voltage of the transformer in the early years of foundation was very low. However, over the time that was along with weakening the coating of the pipelines as well as increasing in resistance in the anodes of the anode-bed which comes from corrosion of the anodes by electrolysis, have caused an increase in the output voltage and current of the transformer. The simulated I_{pv} - V_{pv} and P_{pv} - V_{pv} characteristics of the PV module at different month for a sample of a 295w from Faran Company [20] are shown in Fig. 7.

Table 1. The output voltage and current of the rectifier transformer in a 9-year period

Year	I_{out}	V_{out}	V_{dp}	Year	I_{out}	V_{out}	V_{dp}
2005	1.8	3.98	1.39	2010	4.41	20.7	1.5
2006	2.7	3.88	1.43	2011	5.47	24.53	1.5
2007	2.1	4.21	1.4	2012	5	31.5	1.5
2008	4.23	11.2	1.5	2013	5.56	37.5	1.5
2009	4.1	16.25	1.5				

As shown in Fig. 7 the solar array in the worst climate conditions of December generates a 127w power and in the best climate in July, it can generate a power around 295w. It should be noted that these figures have been achieved by applying the actual data obtained from Meteorological Organization of Ardebil of IRAN to design the PV model.

To optimize the system, first, the calculation of the power generation and consumption during the year is done, and then the number of modules and the batteries are determined with respect to the annual power generation and consumption. Finally, the optimal system is chosen in terms of total cost. These results are given in Table 2 and Table 3. It should be remembered that the excess kWh after charging the batteries are assumed not to be utilized, and, hence, will not actually be produced. If they are produced, they need somewhere to go.

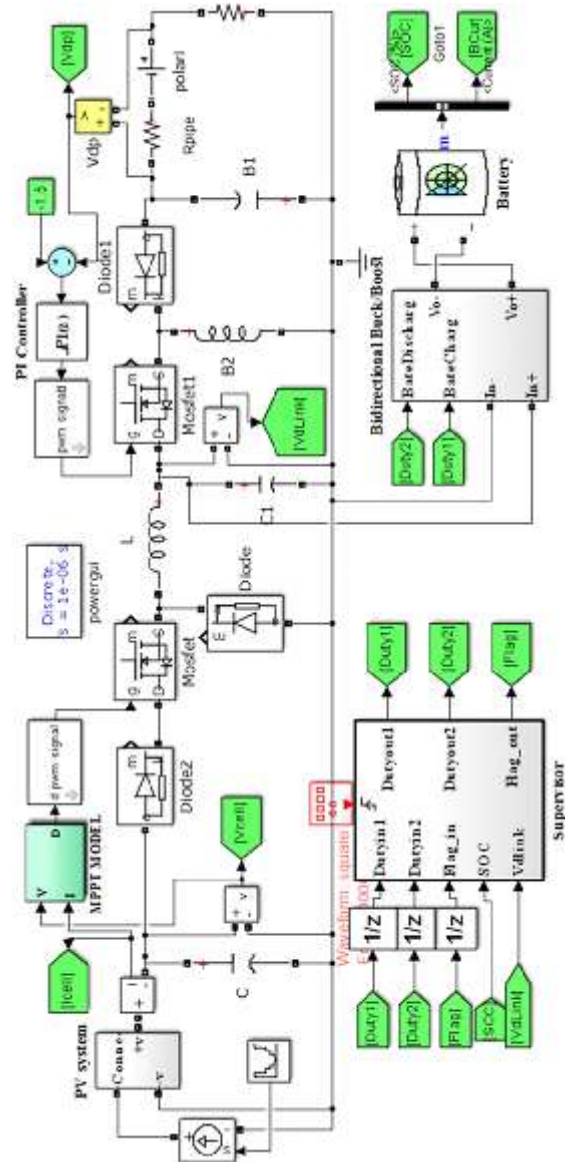


Fig. 8 Simulated model of the system in MATLAB

Table 2 shows the excess monthly kWh produced by the PV array for the 3-module as well as for 4, 5, 6, 7 and 8 modules. The monthly kWh requirements of the batteries can be determined from the months during which the PV excess is negative. All negative excesses represent PV energy shortfalls and thus represent energy to be supplied by the batteries. Before the calculation, a conversion efficiency of 90% is assumed for the buck and buck/boost converters between PV system and the load. The overall efficiency of the bidirectional buck/boost converter for charging and discharging the batteries is assumed about 90% and degradation factor of 0.9 is used for the PV array. Suppose the batteries are allowed to discharge to 10% of full charge. This means that only 80% of the battery rating are available for use and typically 90% of the charging energy can be recovered. In calculation, the number of batteries is rounded up. In

this case, a 1200 Ah, 24 V, 7-year lifetime sealed lead-acid battery costing \$320 is a reasonable choice and the lifetime of the PV modules is assumed to be 20 years. Table 3 shows a trade-off between the purchase of batteries and the purchase of PV modules. Since there is typically more sunlight available in the summer than in the winter, it is possible to configure the battery storage system to store energy from the summer and fall for use in the winter. In addition, it must carefully consider the trade-off between using more batteries, operating at shallower discharge rates to extend the overall life of the batteries vs. using fewer batteries with deeper discharge rates and the correspondingly lower initial cost. In this research, six Poly crystal PV modules are connected as three in parallel sets of two in series from Faran Company [20] because of the constraint of practical size considerations and specifications.

Table 2. Monthly excess kWh capability of PV array for seven array sizes (where A= Number of shiny hours, B= Daily PV power, C= Daily Wh)

Month	A	B	C	Excess kWh (kWh-Needed=150)					
				3mod	4mod	5mod	6mod	7mod	8mod
Apr	6.4	190	1221	-51.1	-18.1	14.8	47.8	81	114
May	7.3	268	1967	9.3	62.4	115.5	168.6	222	275
Jun	10.6	257	2714	69.8	143	216.4	290	363	436
Jul	8.6	295	2549	56.5	125	194.1	263	332	401
Aug	10.7	236	2535	55.3	124	192.2	261	329	397
Sep	6.9	211	1456	-32.1	7.2	46.5	86	125	164
Oct	8.1	152	1236	-49.9	-16	16.8	50	83.6	117
Nov	5.6	152	851	-81.1	-58	-35.1	-12.2	11	33.8
Dec	4	127	508	-109	-95	-81.4	-68	-54	-40.3
Jan	5.8	252	1454	-32.2	7	46.3	86	125	164
Feb	5.7	241	1369	-39.1	-2.2	34.8	72	109	146
Mar	5.2	204	1052	-64.8	-36	-8	20.4	49	77.2
Number of batteries (24v,1200AH)				25	12	7	5	3	2

Table 3. Results of panel size and battery size

Cost	Array					
	3mod	4mod	5mod	6mod	7mod	8mod
Num. Batteries	25	12	7	5	3	2
Battery Cost	8000	3840	2240	1600	960	640
Module Cost	900	1200	1500	1800	2100	2400
Total Cost	8900	5040	3740	3400	3060	3040
Total Cost after 20 years	24900	12720	8220	6600	4980	4320

Five 24 V 1200 Ah industrial batteries are used for this design from Sababattery Company [27] and Electrical characteristic is presented in Table 4.

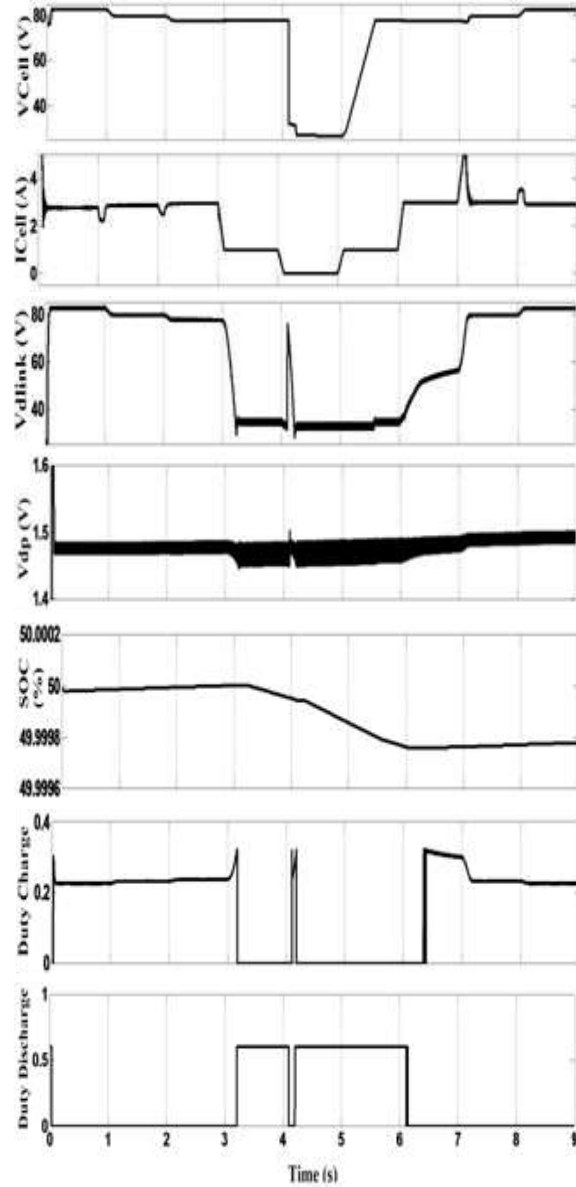


Fig. 9 Simulation results when the Battery works between charging and discharging state freely

Table 4. Electrical characteristic data of 295w PV module (faran co.)

Description	Rating
Rated power	295w
Voltage at maximum power (Vmp)	36.4v
Current at maximum power (Imp)	8.11
Open circuit voltage(Voc)	44.9v
Short circuit current (Isc)	8.55
Storage Temperature	-40 to 85 °C

6. STAND-ALONE SYSTEM SIMULATION

In order to validate the proposed control method, simulations have been carried out using MATLAB/Simulink software as shown in Fig. 8 for time of 9 s.

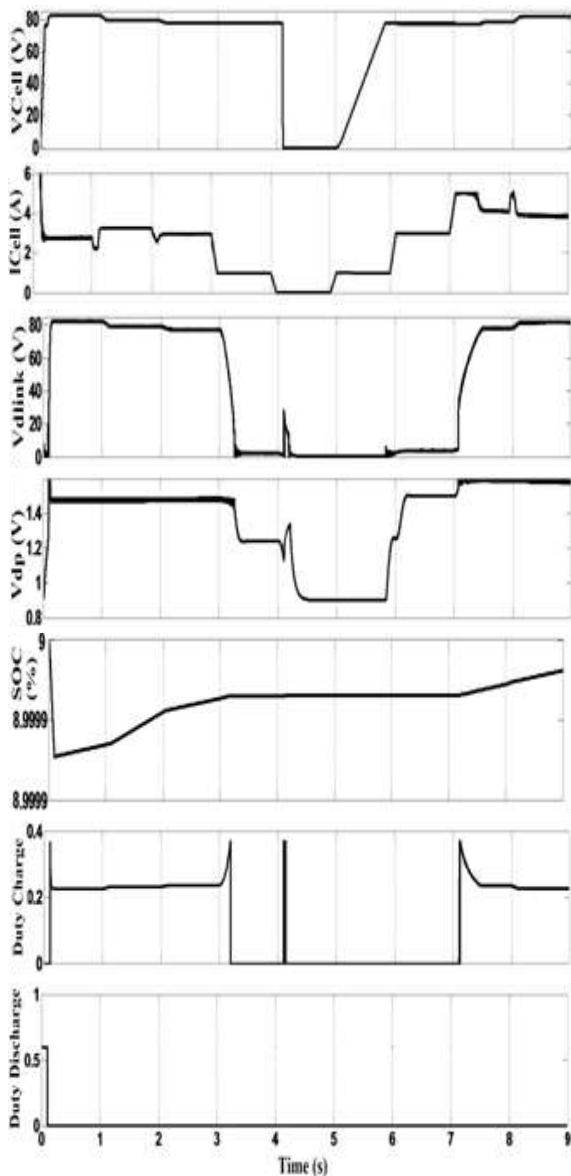


Fig. 10 Simulation results when the battery works only charging state

The reaction of the stand-alone system for different situations is given in Fig. 9 and Fig. 10. As shown in Fig. 8, the simulation blocks consist of the PV generation unit, supervisor, a battery unit, MPPT controller, Buck converter, Buck/Boost converter with PI controller, one bidirectional Buck/Boost converter, and pipeline and anode bed model. In order to study the system's performance during a certain period, in first scenario we assume that the initial SOC of the battery is at 50%, thus the battery can work between charging and discharging state freely. Fig. 9 shows the waveforms of some important point of the system when the solar cell can provide more power than the load needed. The solar irradiation level steps down to reach to zero. After a while, it again steps up to the situation that can provide more power than the load needed. The Vcell and Icell

show the output voltage and current of PV array with the step change of the irradiance, respectively.

It can be observed that the V_{dp} waveform shows that it is well controlled and it is kept at a constant value with acceptable ripple whatever the environmental conditions change; the classic PI regulator rejects these disturbances. It is clear that the voltage variation of V_{dp} in the discharging time of the battery is much higher than in the charging time of the battery but at all both of them is acceptable. The charging and discharging waveforms of the battery show when PV power is greater than load's power, the battery will be charged and during periods of insufficient generation, the battery will provide the shortage energy in order to regulate energy balance.

In the second scenario we assume that the initial SOC of the battery is at 9%, thus the battery can only work in charging state. In addition, the waveform of solar radiation assumed is similar to that of the first scenario. Figure 10 shows the waveforms of some important point of the system. It is observed that the system is not able to maintain the DC link voltage and V_{dp} for the operation mode that the battery cannot provide the energy shortfall.

7. CONCLUSIONS

In this paper, the topology and energy management strategy of a stand-alone photovoltaic power system for cathodic protection of underground pipelines with battery energy storage is proposed. The purpose behind the proposed structure is to design a consistent current source for pipeline while extracting the maximum power from the PV array. Therefore, PV array uses the MPPT control, which can maximize the use of the solar energy. A Modified P&O algorithm has been used to improve dynamic and steady state performance of the MPPT system. The DC link voltage level and the SOC of the battery are employed as an information carrier to represent different operation modes. The battery is connected to the DC link by a ZVS bidirectional Buck/Boost converter to increase the battery lifetime and the system efficiency. The optimal size of the PV array and the battery were determined based on meteorological data, solar irradiance, and the load consumption over a long period to ensure acceptable operation at minimum cost. The MPPT and PI controller of the unidirectional Buck/Boost converter always work independently and the supervisor manages the charge and discharge of the battery. The simulation results have verified that the proposed power management strategy can properly regulate the output voltage and optimal size of the battery plays a vital role in the power management strategy.

REFERENCE

- [1] A.W. Peabody, "Control of pipeline corrosion", by *NACE International Second Edition*, 2001.
- [2] B. Laoun, k.N. boucha, L.serir, "Cathodic protection of a buried pipeline by solar energy", *Revue des Energies Renouvelables*, vol. 12, no.1, pp. 99-104, 2008.
- [3] B James, P.E Bushman, "Corrosion and cathodic protection theory", *Bushman & Associates, Inc.* -P.O. Box 425 - Medina, Ohio 44256 USA.
- [4] Adrian L. Verhiel, "The effects of high-voltage dc power transmission systems on buried metallic pipelines", *IEEE Trans. Ind. Appl.*, vol. 7, no. 3, 1971
- [5] P.R. Mishra, J.C. Joshi, B. Roy, "Design of a solar photovoltaic-power mini cathodic protection system", *Sol. Energ. Mat. Sol. Cells.*, vol. 61, pp. 383-391, 2000.
- [6] R.A. Wagdy, "Design of control circuit of solar photovoltaic powered regulated cathodic protection system", *Sol. Energy*, vol. 55, no.5, pp. 363-365, 1995
- [7] A. A. Ghassami, S. M. Sadeghzadeh, A. Soleimani, "A high performance maximum power point tracker for PV systems" *Int. J. Electr. Power Energy Syst.*, vol. 53, pp. 237-243, 2013
- [8] T. Zhou, W. Sun, "Study on maximum power point tracking of photovoltaic array in irregular shadow," *Int. J. Electr. Power Energy Syst.*, vol. 66, pp. 227-234, 2015.
- [9] N. Ponkarthik, K. Kalidasa Murugavel, "Performance enhancement of solar photovoltaic system using novel maximum power point tracking," *Int. J. Electr. Power Energy Syst.*, vol. 60, pp.1-5, 2014
- [10] A. Murtaza, M. Chiaberge, M. D. Giuseppe, D. Boero, "A duty cycle optimization based hybrid maximum power point tracking technique for photovoltaic systems," *Int. J. Electr. Power Energy Syst.*, vol. 59, pp. 141-154, 2014
- [11] V. Dash, P. Bajpai, "Power management control strategy for a stand-alone solar photovoltaic-fuel cell-battery hybrid system," *Sustainable Energy Technol. Assess.*, vol.9, pp. 68-80, 2015.
- [12] W. Caisheng, H. Nehrir, "Power management of a stand-alone Wind/ Photovoltaic-Fuel cell Energy system," *IEEE Trans. Energy Convers.*, vol.23, no.3, pp.957-67, 2008.
- [13] Y. Hung, Y. Tung, C.H. Chang, "Optimal control of integrated energy management/mode switch timing in a three-power-source hybrid powertrain," *Appl. Energy*, vol.173, pp.184-196, 2016
- [14] J.B. Almada, R.P.S. Leão, R.F. Sampaio, G.C. Barroso, "A centralized and heuristic approach for energy management of an AC microgrid," *Renew. Sustainable Energy Rev.*, vol.60, pp.1396-1404, 2016.
- [15] B.M. Radhakrishnan, D. Srinivasan, "A multi-agent based distributed energy management scheme for smart grid applications," *Energy*, vol. 103, pp.192-204, 2016.
- [16] Z. Liao, X. Ruan, "A novel power management control strategy for stand-alone photovoltaic power system," in *Proc. of the IEEE 6th International Power Electronics and Motion Control Conference*, pp. 445-449, Wuhan, China, 2009.
- [17] K. Sun, L. Zhang, Y. Xing, J. M. Guerrero, "A distributed control strategy based on dc bus signalling for modular photovoltaic generation systems with battery energy storage," *IEEE Trans. Power Electron.*, vol. 26, no. 10, 2011.
- [18] N. Karami, N. Moubayed, R. Outbib, "Energy management for a PEMFC-PV hybrid system," *Energy Conv. Manag.*, vol. 82, pp. 154-168, 2014.
- [19] I. Kashif, S. S. Zainal. "A comprehensive MATLAB simulink PV system simulator with partial shading capability based on two-diode model," *Sol. Energy*, vol.85, pp.2217-2227, 2011.
- [20] Faran Electronic Industries Co. , <http://www.faranco-rp.net>
- [21] R. W. Erickson, D.Maksimovic, "Fundamentals of power electronics second edition", *Publisher Kluwer Academic Publishers* 25/04,2002.
- [22] E. shokati asl; M. Shadnam, M. Sabahi, "High performance Cuk converter considering non-linear inductors for photovoltaic system applications," *J. Oper. Autom. Power Eng.*, vol. 3, no. 2, pp.158-166, 2015.
- [23] A. Pandey, N. Dasgupta, A. K. Mukerjee , "Design issues in implementing MPPT for improved tracking and dynamic performance", in *Proc. of the 32nd Annual Conference on IEEE Industrial Electronics*, pp. 437-439, 2006.
- [24] S. Kharzi, M. Haddadi, A. Malek, "Optimized design of a photovoltaic cathodic protection", *Arab. J. Sci. Eng.*, vol. 34, no. 2B, 2009.
- [25] P. Thounthong, S. Rael, B. Davit, "Control algorithm of fuel cell and batteries for distributed generation system," *IEEE Trans. Energy Convers.*, vol. 23, no. 1, pp. 148-155, 2008.
- [26] F. Boico, B. Lehman, and K. Shujaee, "Solar battery chargers for NIMH batteries," *IEEE Trans. Power Electron.*, vol. 22, no. 5, pp. 1600-1609, 2007.
- [27] Sababattery Company, <http://en.sababattery.ir/>.